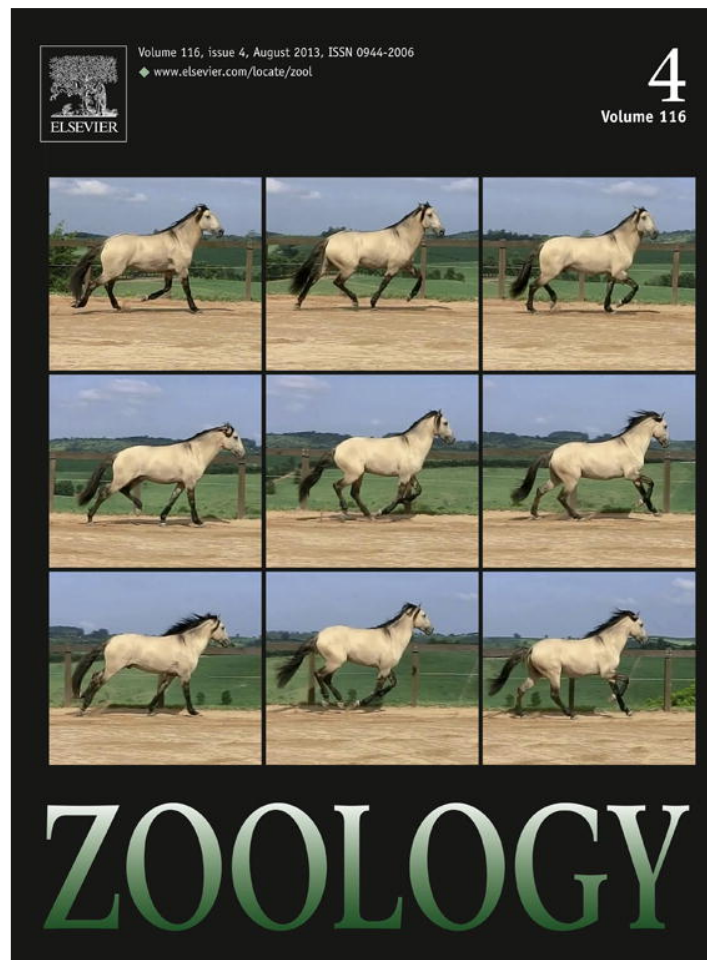


Provided for non-commercial research and education use.
Not for reproduction, distribution or commercial use.



This article appeared in a journal published by Elsevier. The attached copy is furnished to the author for internal non-commercial research and education use, including for instruction at the authors institution and sharing with colleagues.

Other uses, including reproduction and distribution, or selling or licensing copies, or posting to personal, institutional or third party websites are prohibited.

In most cases authors are permitted to post their version of the article (e.g. in Word or Tex form) to their personal website or institutional repository. Authors requiring further information regarding Elsevier's archiving and manuscript policies are encouraged to visit:

<http://www.elsevier.com/authorsrights>



Contents lists available at SciVerse ScienceDirect

Zoology

journal homepage: www.elsevier.com/locate/zool

ZOOLOGY

A revised metric for quantifying body shape in vertebrates

David C. Collar^{a,*}, Crystal M. Reynaga^a, Andrea B. Ward^b, Rita S. Mehta^a

^a Department of Ecology and Evolutionary Biology, Long Marine Laboratory, University of California, 100 Shaffer Road, Santa Cruz, CA 95060, USA

^b Department of Biology, Adelphi University, Garden City, NY 11530, USA

ARTICLE INFO

Article history:

Received 23 August 2012

Received in revised form 9 February 2013

Accepted 20 March 2013

Available online 27 May 2013

Keywords:

Axial skeleton

Body shape diversity

Comparative anatomy

Elongation

Locomotion

ABSTRACT

Vertebrates exhibit tremendous diversity in body shape, though quantifying this variation has been challenging. In the past, researchers have used simplified metrics that either describe overall shape but reveal little about its anatomical basis or that characterize only a subset of the morphological features that contribute to shape variation. Here, we present a revised metric of body shape, the vertebrate shape index (VSI), which combines the four primary morphological components that lead to shape diversity in vertebrates: head shape, length of the second major body axis (depth or width), and shape of the precaudal and caudal regions of the vertebral column. We illustrate the usefulness of VSI on a data set of 194 species, primarily representing five major vertebrate clades: Actinopterygii, Lissamphibia, Squamata, Aves, and Mammalia. We quantify VSI diversity within each of these clades and, in the course of doing so, show how measurements of the morphological components of VSI can be obtained from radiographs, articulated skeletons, and cleared and stained specimens. We also demonstrate that head shape, secondary body axis, and vertebral characteristics are important independent contributors to body shape diversity, though their importance varies across vertebrate groups. Finally, we present a functional application of VSI to test a hypothesized relationship between body shape and the degree of axial bending associated with locomotor modes in ray-finned fishes. Altogether, our study highlights the promise VSI holds for identifying the morphological variation underlying body shape diversity as well as the selective factors driving shape evolution.

© 2013 Elsevier GmbH. All rights reserved.

1. Introduction

Body shape is one of the most prominent axes of morphological diversity among vertebrates. Within the major higher-level taxa, shape variation can be characterized as a continuum extending from short, stout forms at one extreme to long, skinny bodies at the other. Ray-finned fishes, for example, vary from disc-like (e.g., flatfish, ocean sunfish) or football-shaped (e.g., pufferfish) to eel-like forms (e.g., true eels, eelpouts, pricklebacks). Lissamphibians (i.e., extant members of Amphibia) range in shape from compact (e.g., frogs and toads) to highly elongate (e.g., sirens, caecilians). Squamata include both stout-bodied (e.g., horned lizards) and snake-like lizards (e.g., amphisbaenids, glass lizards) as well as snakes. In Mammalia and Aves, overall body shape variation may take a backseat to cranial and appendicular diversity, but these groups also show marked variation along the elongation continuum (e.g., terrestrial vs. marine ungulates, diving vs. perching birds).

This diversity in body shape has long captivated functional and comparative morphologists because the shape of an organism's

body affects many aspects of its biology. In fishes and tetrapods, body shape is related to axial flexibility and locomotor performance (Lindsey, 1975, 1978; Webb, 1982; Brainerd and Patek, 1998; Porter et al., 2009), which in turn determines suitable microhabitats (Nelson, 2006). For example, extreme elongation in fishes may confer flexibility and maneuverability that allow occupation of narrow crevices, as seen in elongate gobies living in the interstitial habitat of gravel beaches (Yamada et al., 2009). In addition, the degree of body elongation influences gut morphology (Ward and Kley, 2012) and imposes structural constraints on elements of the feeding apparatus, thereby affecting feeding physiology and ecology (Gans, 1975; Pough et al., 1998). Body shape may even have consequences for diversification of evolutionary lineages (Bergmann and Irschick, 2012).

Despite widespread interest in body shape and its functional, ecological and evolutionary consequences, no consensus or unifying metric has emerged for quantifying shape. Many previous researchers have summarized morphological shape variation using multivariate statistical approaches, such as principal components or discriminant function analysis (e.g., Losos, 1990; Walker and Bell, 2000; Rüber and Adams, 2001; Langerhans et al., 2007; Brandley et al., 2008; Adams et al., 2009; Bergmann et al., 2009). In particular, landmark-based morphometrics, a method of quantifying shape

* Corresponding author. Tel.: +1 5302200110.

E-mail address: dccollar@gmail.com (D.C. Collar).

variation among taxa based on deviations in a series of landmarks spread across the body, has been highly effective at identifying aspects of shape that differentiate taxa (see reviews in Rohlf and Marcus, 1993; Adams et al., 2004). However, this method may have only limited utility for quantifying broad scale patterns of vertebrate shape diversity because the variety of forms that can be included in the analysis may be restricted by the presence of homologous structures and landmarks. In addition, aspects of body shape that load strongly on the resulting principal components or canonical axes depend on the sample of taxa and traits included in the study. This sample dependence makes it difficult to compare shape variation across studies, particularly when sampled taxa differ substantially in variability among species, possess different structures, or have been preserved or measured in different ways.

An alternative approach to the application of multivariate statistics has been to devise and apply metrics that combine body measurements in ways that capture variation along the elongation continuum. Several simple metrics involve the ratio of an organism's anterior–posterior length to its second longest axis (dorso-ventral depth or lateral width), including elongation ratio (ER = standard length/second longest body axis, where standard length is an ichthyological measure of body length that excludes the caudal fin rays; Ward and Azizi, 2004), fineness ratio (FR = total body length/body depth; Webb, 1975), and body aspect ratio (BAR = total body length/body width; Helfman et al., 2009). The latter two were originally designed to relate body shape to swimming performance, but all three metrics can be applied to describe shape for almost any vertebrate taxon such that more elongate species have larger values. These ratios, however, provide only limited insight into the morphological basis of shape variation, and identification of underlying structural differences requires collection of more detailed anatomical measurements.

Body shape transformations along the elongation continuum may result from modifications of several morphological components. Many studies have shown that highly elongate vertebrates have more vertebrae when compared to closely related non-elongate species (Wake, 1966; Lindsey, 1975; Asano, 1977; reviewed in Richardson et al., 1998; Polly et al., 2001; Ward and Brainerd, 2007), though elongate species may differ in the region of the axial skeleton showing increased vertebral numbers (Polly et al., 2001; Ward and Brainerd, 2007; Mehta et al., 2010; Müller et al., 2010; Ward and Mehta, 2010). In addition, many elongate forms are known to exhibit increased length of the individual vertebrae (Johnson, 1955; Wake, 1966; Parra-Olea and Wake, 2001; Polly et al., 2001). To incorporate these possible modifications of the axial skeleton into a metric of elongation, Ward and Brainerd (2007) proposed the axial elongation index (AEI), which combines measurements of vertebral number and shape in the abdominal and caudal regions. Similar to the simpler elongation metrics, AEI varies such that greater values characterize more elongate species, but analysis of the components of AEI can also reveal what aspects of the axial skeleton are responsible for body elongation (Ward and Brainerd, 2007; Yamahira and Nishida, 2009; Ward and Mehta, 2010; Mehta et al., 2010). Although the development of the AEI is a step toward elucidating the morphological basis of body shape variation, it captures only a subset of the features that can underlie shape differences. In addition to the shape of the axial skeleton, vertebrates also vary in relative head size and shape and in relative length of the second major body axis (Ward and Mehta, 2010; Mehta et al., 2010) (see Fig. 1).

Here, we offer a revised metric for quantifying body shape, the vertebrate shape index (VSI), which combines the four major anatomical components that contribute to body shape variation among vertebrates:

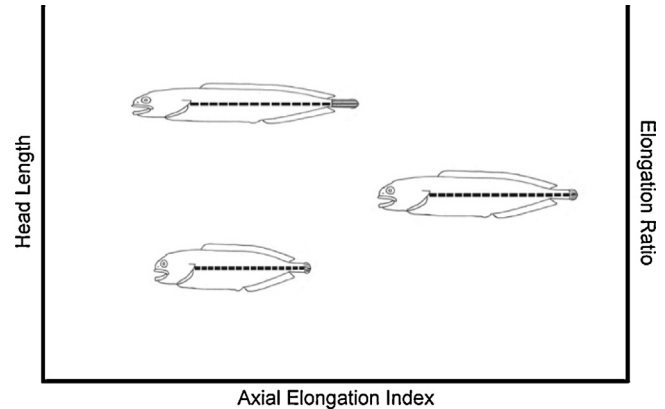


Fig. 1. Hypothetical distribution of body shapes in a morphospace defined by axial elongation index (AEI), head length (HL), and elongation ratio (ER). Relative length of the head or secondary body axis may vary independently of elongation in the axial skeleton, resulting in a weak correlation between commonly used metrics of body shape – AEI and ER. Line drawings are of a general eelpout (Zoarcidae).

$$VSI = \text{secondary axis reduction} + \text{head elongation} + \text{precaudal elongation} + \text{caudal elongation} \quad (1)$$

Secondary axis reduction is the anterior–posterior length of the body (L_{axis1}) relative to the length of the secondary body axis (the greater one of body depth or width, L_{axis2}) and is equivalent to ER. *Head elongation* is the product of head length, quantified as the number of vertebrae spanning the antero-posterior length of the head ($L_{head \text{ in vertebrae}}$), and head aspect ratio (AR_{head}), which is the ratio of head length to its length in the dimension of the secondary body axis (i.e., dorso-ventral depth, if the secondary body axis is depth, or lateral width, if the secondary body axis is width; see Section 2.2). *Precaudal and caudal elongation* follow the formulation in Ward and Brainerd's (2007) work on the AEI, where *precaudal elongation* equals the product of the number of precaudal vertebrae (N_{PCV}) and the mean aspect ratio of precaudal vertebrae (AR_{PCV}), and *caudal elongation* is the product of the number of caudal vertebrae (N_{CV}) and the mean aspect ratio of caudal vertebrae (AR_{CV}) (see Section 2.1 for justification of morphological traits included in VSI and the mathematical functions for combining them). Vertebral aspect ratios are calculated in the same way as head aspect ratio: antero-posterior length divided by either depth or width depending on the secondary body axis. Combining all of these terms,

$$VSI = \left(\frac{L_{axis1}}{L_{axis2}} \right) + (L_{head \text{ in vertebrae}} \times AR_{head}) + (N_{PCV} \times AR_{PCV}) + (N_{CV} \times AR_{CV}) \quad (2)$$

We intend for VSI to be a metric of body shape that varies between highly elongate forms at large values and stout forms at small values. Moreover, because the morphological features that comprise VSI are shared by all vertebrate taxa, VSI can be calculated for any vertebrate and analyzed in a way that allows for identification of the structural changes leading to body shape diversity.

In the present study, we demonstrate the utility of VSI through four primary objectives. (i) We quantify VSI for a diverse sample of 194 vertebrates and estimate VSI diversity within five major vertebrate clades: Actinopterygii, Lissamphibia, Aves, Squamata, and Mammalia. (ii) We describe how the components of VSI can be measured for a variety of specimen preparations. Vertebrate taxa differ in the techniques commonly used to reveal skeletal structures, such

as clearing and staining (used predominantly on small vertebrates), dry skeletal preparation and radiography, and we detail methods for making homologous measurements on each specimen type. (iii) To assess the importance of VSI's morphological components to shape variation, we quantify their independent contributions to VSI diversity as well as their degree of correlation within vertebrate clades. This aspect of our study illustrates how VSI can be used to identify the anatomical basis of body shape variation and serves to evaluate VSI as a revision of AEI. Because VSI is simply the sum of secondary axis reduction, head elongation and AEI, the revision is only necessary if secondary axis reduction and head elongation are important independent contributors to shape variation. (iv) We demonstrate how VSI can be applied to questions in comparative and functional anatomy by testing a hypothesized relationship between VSI and degree of axial bending during swimming in ray-finned fishes.

2. Materials and methods

2.1. Rationale for VSI's formulation

VSI additively combines the shape of four major anatomical regions known to contribute to variation along the elongation continuum in vertebrates: secondary body axis reduction, head elongation, and elongation of both precaudal and caudal regions of the vertebral column. We quantify the shape of each of these regions such that more elongate forms have larger values. To avoid confounding variation in VSI and its components with variation in size, we use ratios to describe the lengths of structures relative to their lengths in the dimension of the secondary body axis. We choose this method over other methods that account for size, such as linear regression against a size variable, for two reasons. First, we want VSI to be a metric that can be calculated for any specimen directly from measurements of its morphology. Second, we want a specimen's VSI to be stable (i.e., invariant across studies), and many size correction methods, including regression, give values for taxa that depend on the sample of species included in the analysis. These considerations are made with the overall goal of allowing VSI measurements from multiple studies to be readily combined. Below we describe our rationale behind the formulae combining morphological measurements to determine each of VSI's components (see Eq. (2)).

We quantify *secondary axis reduction* as ER because this variable describes the relative lengths of the body in its primary and secondary dimensions in a manner that gives larger values for more elongate forms.

Head elongation combines head length relative to the length of the axial skeleton and the degree of head lengthening in the antero-posterior dimension relative to its depth or width (i.e., AR_{head}). We quantify relative head length as $L_{head\ in\ vertebrae}$ because standardizing by the number of vertebrae equivalent to head length ensures head elongation will be of similar magnitude to *precaudal elongation* and *caudal elongation*. In contrast, standardizing head length by body length would result in a relative head length value less than 1 and would diminish the contribution of head elongation to VSI. Multiplying $L_{head\ in\ vertebrae}$ by AR_{head} provides a description of the degree of head elongation that is comparable to the degree of axial skeletal elongation.

Following Ward and Brainerd (2007), *precaudal* (or *caudal*) *elongation* is the product of the N_{PCV} (or N_{CV}) and mean AR_{PCV} (or AR_{CV}) of individual vertebrae within that region. Because aspect ratio describes the relative lengthening of the vertebrae, multiplying this value by the number of vertebrae gives a size-standardized description of the degree of elongation of each axial region.

2.2. Taxonomic sampling

We sampled vertebrate species spanning the elongation continuum to assess whether VSI separates stout-bodied from elongate species as we intended. Specimens came from personal collections and from the collections of Mammalogy and Ornithology at the Natural History Museum of Los Angeles County and Herpetology and Ichthyology at the California Academy of Sciences (for museum accession numbers, see Table S1 in the supplementary online Appendix A). We collected body shape data from a total of 194 species spread across seven major clades (Actinopterygii, $n = 117$; Lissamphibia, $n = 14$; Testudines, $n = 3$; Squamata, $n = 14$; Crocodylia, $n = 2$; Aves, $n = 11$; Mammalia, $n = 33$). Within each clade we targeted species at the extremes of the elongation continuum and opportunistically sampled species with intermediate body shapes. In addition, a large portion of our sampling of Actinopterygii came from the highly elongate Anguilliformes (true eels, $n = 36$) and the highly shape-variable Blennioidei (blennies, kelpfish, stargazers and allies, $n = 32$). Focusing on these groups allowed us to assess the anatomical basis of body shape variation at a finer taxonomic level than the more inclusive vertebrate clades permitted. Whenever possible we examined multiple adult individuals per species (min. = 1; max. = 8), and species values were taken as the means of measurements from individual specimens. Because specimen preparations vary across vertebrate taxa, we examined cleared and stained specimens, dry skeletal preparations, and radiographs. In Section 2.3 we detail our methods for measuring VSI's morphological variables. Depending on the size of the specimens, measurements were taken using measuring tape to the nearest 0.1 mm or analog calipers recorded to the nearest 0.01 mm.

2.3. Morphological measurements

Primary body axis length (referred to throughout simply as body length), L_{axis1} , is the distance from the anterior-most point of the skull to the posterior end of the vertebral column. This variable is equivalent to the commonly used ichthyological body size measurement, standard length, which excludes the length of the caudal fin rays. Body length can be readily measured on any vertebrate skeletal preparation, though some caution is required to exclude specimens with breaks in the caudal axial skeleton, which may be common in squamates and salamanders that autotomize their tails.

Secondary body axis length, L_{axis2} , is the greater one of dorso-ventral body depth and lateral width. Body depth is measured perpendicular to the primary body axis at the point where the distance between the dorsal and ventral surfaces is greatest posterior of the skull. These surfaces are intact on cleared and stained specimens, but for skeletons or radiographs, which lack the body wall, measurements must be made between skeletal elements. In many vertebrates, body depth is the vertical distance between the dorsal-most point of the vertebral neural arch and the ventral-most point of the rib at the postcranial skeleton's deepest point. However, in many ray-finned fishes, post-cranial skeletal elements lie above the neural arch or below the distal end of the ribs (e.g., pterygiophores, pelvic girdle). This measurement may, for example, be taken between the dorsal- and ventral-most points on the pterygiophores supporting the dorsal and anal fins, or between the dorsal pterygiophores and the ventral-most aspect of the pelvic girdle. Body depth does not include dorsal or anal fins of fishes. Body width is measured perpendicular to the primary body axis and is the distance between the left and right body surfaces at their widest point. On skeletal preparations and radiographs, body width is the distance between the left- and right-most extensions of the ribs. Radiographs, of course, contain only two dimensions, one of which is the primary body axis. As long as the second dimension includes the secondary body axis, these preparations will be appropriate

for VSI measurements. However, if it is unclear that a radiograph contains the secondary body axis, we recommend against using it because its VSI may not be comparable to VSI values determined from three-dimensional specimens.

The secondary body axis determines the second dimension (i.e., denominator) for head and vertebral aspect ratios. This approach effectively describes specimens in only two dimensions – the primary and secondary body axes. For some specimens, the secondary axis of the head or vertebrae will not be in the dimension of the secondary body axis (e.g., the secondary body axis is depth, but head width is greater than head depth). But even in these cases, the denominator for aspect ratio is measured in the dimension of the secondary body axis. This strategy ensures that all morphological variables comprising VSI correspond between three-dimensional specimen preparations, such as cleared and stained specimens, and two-dimensional preparations, such as radiographs.

Head length standardized by vertebral length, $L_{head\ in\ vertebrae}$, is evaluated as the linear span of the skull along the primary body axis divided by the average vertebral length, which is the mean of region-specific vertebral lengths weighted by regional vertebral counts (see below).

Head aspect ratio, AR_{head} , is the ratio of head length (as a measured distance, not standardized by vertebral length) to its length in the dimension of the secondary body axis. Head depth and width are measured in a manner similar to body depth and width, at the deepest and widest points along the skull.

Regional vertebral counts, N_{PCV} and N_{CV} , require elaboration because vertebrate taxa vary in the degree of differentiation along the axial skeleton (Fig. 2). We divided the vertebral column into regions shared across vertebrate groups: precaudal and caudal. The precaudal region is the portion of the vertebral column lacking fused haemal arches, whereas the caudal region contains vertebrae with fused haemal arches (Grande and Bemis, 1998; Ward and Brainerd, 2007). Actinopterygians possess only these two regions (Grande and Bemis, 1998), while other vertebrates show a greater degree of regionalization. In all cases, though, the enhanced differentiation is contained within the precaudal region. Birds and mammals possess four precaudal regions – cervical, thoracic, lumbar, and sacral. Lissamphibians and squamates have three precaudal regions – cervical, thoracolumbar, and sacral (Pough et al., 2009). Precaudal vertebral counts, N_{PCV} , were taken as the sum of all differentiated precaudal regions. For each specimen, regional vertebral counts were taken as the mean of three separate counts.

Regional vertebral aspect ratios, AR_{PCV} and AR_{CV} , are the ratios of vertebral centrum antero-posterior length to length in the dimension of the secondary body axis. For each specimen, we measured aspect ratios for three haphazardly selected vertebrae spread across all vertebral regions and evaluated AR_{PCV} and AR_{CV} as the means of these measurements. In taxa with differentiated precaudal vertebrae, we measured aspect ratios for three vertebrae from each precaudal region and evaluated AR_{PCV} as the mean of region-specific aspect ratios weighted by the number of vertebrae within each region. Although this method may result in a loss of information about vertebral shape in some taxa, it permits comparisons among groups with and without differentiation of the precaudal region.

2.4. Estimating diversity within vertebrate clades

To determine whether VSI does in fact separate elongate and stout shapes, we quantified body shape diversity as the ranges of VSI and its anatomical components within each of five major clades of vertebrates – Actinopterygii, Lissamphibia, Aves, Mammalia, and Squamata. We excluded Testudines and Crocodylia from this analysis because of limited sample size. We avoided statistical comparisons among clades and applied range rather than variance as a metric of diversity because our sampling targeted species at the

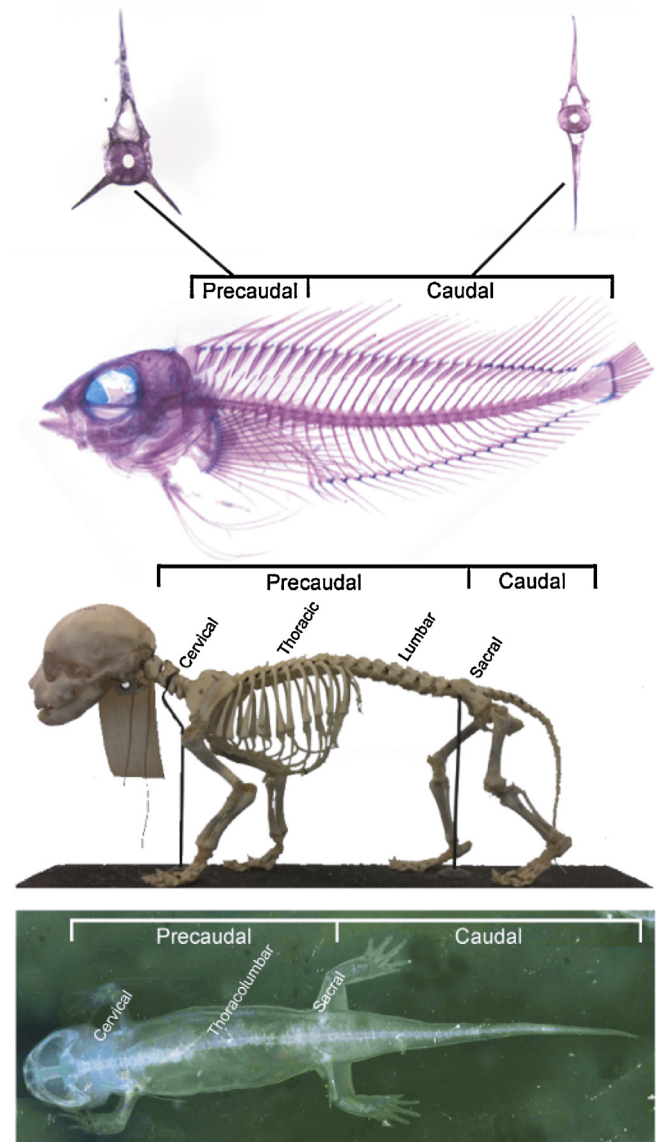


Fig. 2. Illustration of various specimen preparations used to compile this data set and the differences in vertebral regionalization of ray-finned fishes, mammals, and lissamphibians. (A) Cleared and stained specimen of rosy blenny (*Malacoctenus macropus*). Ray-finned fish specimens are often cleared and stained. They have only two vertebral regions – precaudal and caudal, defined by the absence and presence, respectively, of a fused haemal arch. (B) Articulated skeleton of a juvenile lion (*Felis leo*). All mammal specimens we measured were skeletonized. Mammals (along with Aves, not pictured) have the greatest degree of vertebral differentiation with four distinct precaudal regions – cervical, thoracic, lumbar, and sacral – plus caudal vertebrae. (C) Radiograph of Pacific giant salamander (*Dicamptodon ensatus*). Many lissamphibian specimens were X-rayed. Lissamphibians (and squamates, not shown) have an intermediate degree of axial regionalization with three precaudal regions – cervical, thoracolumbar, and sacral – in addition to caudal vertebrae.

extremes of the body elongation continuum and sparsely sampled intermediate forms relative to their actual abundance within vertebrate groups. This sampling strategy inflates the variance because extreme forms are overrepresented, but the range should remain relatively unchanged with more extensive sampling as long as we have included forms near the extremes. Nevertheless, these comparisons of body shape ranges are intended as a heuristic exercise to highlight potential questions to which VSI can be applied. Because VSI can be measured for any vertebrate, it allows examination of body shape variation – however quantified – along a single axis among any sample of taxa.

2.5. Quantifying the contributions of VSI components to shape variation

To assess the importance of the four anatomical components of body shape diversity, we examined their independent contributions to VSI variation within five major vertebrate clades (as above, Testudines and Crocodylia were excluded from this analysis because of small sample size). We applied multiple linear regression of VSI against secondary axis reduction, head elongation, precaudal elongation, and caudal elongation separately within each clade. Because VSI is calculated directly as the sum of the four anatomical components (see Eq. (1)), there is no residual variation. Rather than test the statistical significance of the regression model, our goal was to partition the variation in VSI among its components and assess their independent contributions, quantified as the marginal (Type III) sums of squares relative to the total sum of squared deviations in VSI. We also quantified the proportion of variation in VSI that is shared among components as the difference between the total sum of squares for VSI and the sum of marginal sums of squares for all components. Multiple linear regression models were fit using least squares implemented in the function *lm* in the R statistical computing environment (R Development Core Team, 2012).

We evaluated the degree of correlation among secondary axis reduction, head elongation, precaudal elongation, and caudal elongation. Within each of the five major vertebrate clades sampled, we estimated Pearson correlation coefficients for all pairwise combinations of components using the *cor* function in R (R Development Core Team, 2012). In combination with the multiple linear regressions, these between-component correlations served to validate (or invalidate) the inclusion of each of the four components that comprise VSI; low correlations indicate a large degree of independent contributions to VSI, while high correlations suggest that some components are redundant.

We applied multiple regression and correlation analysis to the two more densely sampled ray-finned fish clades, Anguilliformes and Blennioidei. Focusing on Anguilliformes allowed us to assess the anatomical basis of body shape variation within a clade whose species occupy the elongate extreme of the body shape continuum. Blennioidei permitted investigation into what components underlie differences in body shape in a clade that includes a wide range of shapes, from relatively short-bodied to highly elongate species.

2.6. Examining the relationship between VSI and locomotor mode in ray-finned fishes

To illustrate how VSI can be applied to examine the biological consequences of body shape variation, we asked whether an association exists between VSI and locomotor mode in Actinopterygii. We evaluated the hypothesis that body elongation enhances axial bending and body undulation-based swimming and tested whether VSI is greater in species that employ a large degree of axial bending during steady swimming. For a subset of our sampled ray-finned fishes, we assigned species to one of four general swimming modes: paired fin propulsion (labriform and diodontiform swimming), median fin propulsion (amiiform swimming), caudal undulation (carangiform, subcarangiform and thunniform swimming), and body undulation (anguilliform swimming) (Liem et al., 2001; Helfman et al., 2009). We selected a phylogenetically dispersed sample of species to represent each swimming mode. Assignments of swimming mode to species were based on personal observation, and species whose swimming modes were uncertain to us or did not fit within a single category were excluded from this analysis. For some modes our data set included multiple species from the same family or order, which likely share a swimming mode by common descent (Anguilliformes [$n=36$], Labridae [$n=3$], Ophidiiformes [$n=3$ for fin-based propulsors],

Salmoniformes [$n=2$], and Stichaeidae [$n=2$]). Because inclusion of all species from the same family or order would lead to phylogenetic bias and pseudoreplication, we evaluated the mean value for each higher taxon and used the mean as a single sample in the ANOVA. Our data set therefore included means for higher taxa and species values for species sampled from distantly related taxa. This sampling strategy resulted in the following sample sizes within swimming modes: n (paired fin propulsors)=4 taxa (3 species + 1 family mean), n (median fin propulsors)=3 taxa (2 species + 1 order mean), n (caudal undulators)=4 species; n (body/caudal undulators)=4 taxa (2 species + 1 order mean + 1 family mean). Additional information on taxonomic sampling within swimming modes is provided in Table S2 in the supplementary online Appendix A.

We used ANOVA and one-tailed Tukey's HSD tests, implemented in the functions *aov* and *TukeyHSD* in R (R Development Core Team, 2012), to evaluate the statistical significance of differences among swimming modes. We tested the prediction that body undulators have the highest VSI, paired fin propulsors have the lowest VSI, and caudal undulators and median fin propulsors exhibit intermediate VSI values. We were unable to predict, however, whether caudal undulators or median fin propulsors would be more elongate. On the one hand, caudal undulators generate axial bending during swimming, but on the other hand, median fin propulsors may expand the area of the propulsive surface – the confluent median fin – by lengthening the postcranial skeleton (Ward and Mehta, 2010).

2.7. Note on the use of non-phylogenetic statistical methods

Our statistical analyses did not account for phylogenetic relatedness and thus assumed that data from species are independent. Although these non-phylogenetic methods may be appropriate when phenotypic similarity is uncorrelated with shared evolutionary history (i.e., low phylogenetic signal; Blomberg et al., 2003; Freckleton et al., 2002), we do not argue that such is the case for our data. In fact, we suspect at least a moderate amount of phylogenetic signal in our data, given our attempts to sample several species at the extremes of the elongation continuum within major vertebrate clades. In some cases, these species are more closely related to one another than other species within the clade (e.g., anguilliform eels within Actinopterygii, anurans within Lissamphibia). Our goal, however, was simply to illustrate the ways in which VSI can be applied to study body shape diversity, and we chose non-phylogenetic statistics to avoid excluding large amounts of data for species not found in published phylogenies. In addition, we sought to avoid complicating the presentation of VSI with our own phylogenetic analyses of the species in our sample.

The potential problems associated with neglecting phylogenetic relatedness are likely to be most relevant to our multiple linear regressions of VSI against its anatomical components and the estimation of correlation coefficients for pairs of VSI components. We sought to minimize the potential influence of phylogenetic non-independence on comparisons of VSI and its components among actinopterygian swimming modes by sampling species from a variety of families and orders (see above). Phylogenetic relationships among these taxa may nevertheless influence the ANOVA. Non-phylogenetic methods are prone to inflated Type I error rates (Felsenstein, 1985) and elevated variance in parameter estimation (Rohlf, 2006) relative to phylogenetic methods when phylogenetic signal is high. We therefore avoid making strong inferences about statistical significance of estimated parameters and instead view these results as illustrative of the potential insights VSI can provide. We note that future statistical analyses of VSI should involve phylogenetic methods whenever possible.

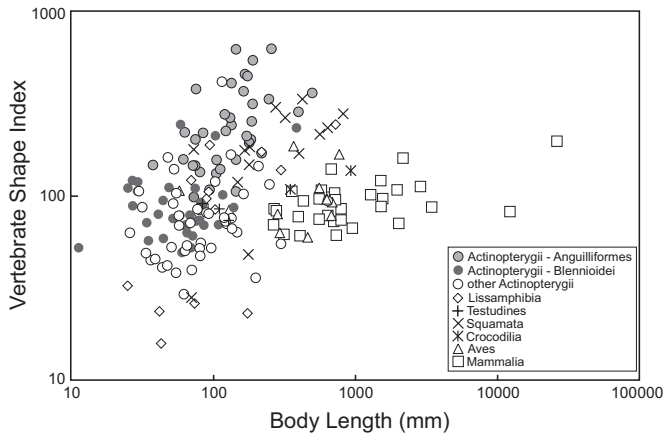


Fig. 3. Scatterplot of the vertebrate shape index (VSI) against body length (distance in mm between the anterior tip of the skull and the posterior-most point of the axial skeleton) on log-scale axes for 194 species of vertebrates. Shapes represent vertebrate clade identity, and within Actinopterygii, shading indicates whether species belong to Anguilliformes (true eels), Blennioidei (blennies, kelpfishes, stargazers), or other ray-finned fish groups.

3. Results

3.1. VSI diversity and its anatomical basis in vertebrate clades

To highlight that VSI can be applied to quantify body shape variation along the elongation continuum, we examined VSI values for species from seven major vertebrate clades. Within five of these clades (Actinopterygii, Lissamphibia, Squamata, Aves and Mammalia), we estimated the range of VSI among species and quantified the independent contributions of anatomical components to VSI diversity. Crocodylians and turtles are represented by too few species to be included in these analyses, but we note that the sampled species of both clades fall in the middle of the VSI range for all vertebrates (Fig. 3). Below, we describe results from each of the more densely sampled clades, proceeding from the most to the least diverse.

Actinopterygii: Ray-finned fishes span the largest range of VSI – 1.3 orders of magnitude (Table 1), nearly the entire range for all the vertebrates in our data set (Fig. 3). At the lower VSI extreme are several deep-bodied coral reef fishes (tang/*Zebraflorea flavescens*, VSI = 29.3; butterflyfish/*Chaetodon multicinctus*, VSI = 39.6; pufferfish/*Sphoeroides maculatus*, VSI = 41.8) as well as the disc-shaped scat (*Scatophagus argus*, VSI = 38.1), pompano (*Trachinotus blochii*, VSI = 35.8) and the wedge-shaped hatchetfish (*Gasteropelecus sternicla*, VSI = 40.8). The upper extreme of the VSI continuum is made up mostly of anguilliform fishes (true eels), including the species with the largest VSI value in our data set, the ribbon moray (*Rhinomuraena quaesita*, VSI = 622.7), but also the long, stiffer-bodied needlefish (*Strongylura marina*, VSI = 413.8) and some elongate blennioids (stargazer/*Myxodagnus opercularis*, VSI = 242.3; hairtail blenny/*Xiphiasia setifer*, VSI = 232.8; tube blenny/*Chaenopsis alepidota*, VSI = 210.9). Notably, the needlefish has the eighth largest VSI, which seems to be a result of its head elongation (=303.4) far exceeding the values of all other vertebrates in our data set.

Caudal elongation is the greatest independent contributor to VSI variation in ray-finned fishes (21%), though the majority of shape variation is shared among anatomical components (65%; Fig. 4). This latter result is a consequence of the substantial correlation among three of the four morphological components within ray-finned fishes. Consistent with previous work examining body shape diversity in fishes (Lindsey, 1975; Ward and Brainerd, 2007; Ward and Mehta, 2010), we found strong positive correlations between precaudal elongation and caudal elongation ($r = 0.68, P < 0.001$), and

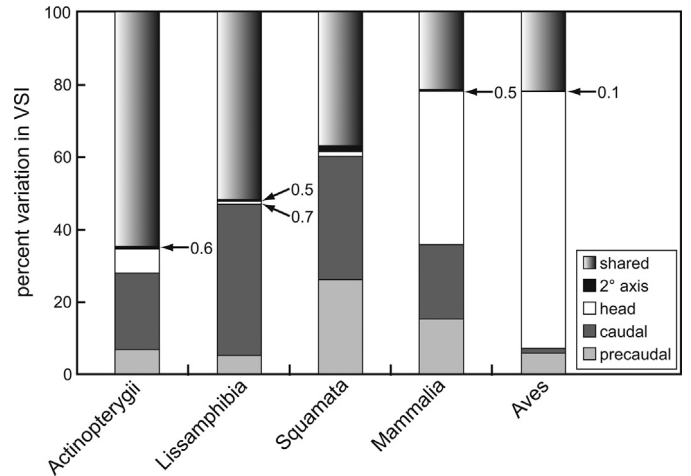


Fig. 4. Partitioning the independent contributions of secondary axis reduction (2° axis), head elongation (head), precaudal elongation (precaudal), and caudal elongation (caudal) to VSI variation within each of five vertebrate clades. Bars represent the percentage of the total sum of squared deviation in VSI that is explained independently by each component, quantified as its marginal (Type III) sum of squares. The shared component is the percentage of variation in VSI explained by more than one component. Arrows and corresponding values indicate the percent of variation explained by components whose bar heights are shorter than 2%.

between secondary axis reduction and elongation of both vertebral regions (secondary axis reduction and precaudal elongation: $r = 0.49, P < 0.001$; secondary axis reduction and caudal elongation: $r = 0.35, P < 0.001$; Table 2). Although it accounts for a modest proportion of VSI variation (7%; Fig. 4), head elongation is only weakly correlated with the other components (Table 2) and seems to be an independent axis of shape variation in ray-finned fishes.

Within the more densely sampled subclasses of Actinopterygii – Anguilliformes and Blennioidei – caudal elongation is the most important independent explanatory variable of VSI (36 and 16%, respectively; Fig. 5). Precaudal elongation also accounted for a substantial proportion of variation in Anguilliformes (13%), but

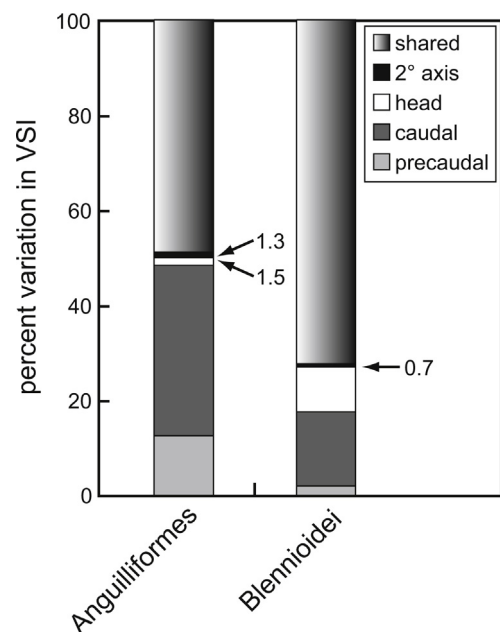


Fig. 5. Partitioning the independent contributions of VSI components in two subclasses of ray-finned fishes – Anguilliformes (true eels) and Blennioidei (blennies, kelpfishes, stargazers, and allies). See legend of Fig. 4 for details on what bar height represents.

Table 1
Minimum (min.) and maximum (max.) values for VSI and its anatomical components within each of five major vertebrate clades.

Trait	Group	Min.	Min. species	Max.	Max. species	Range ^a
VSI	Actinopterygii	29.26	<i>Zebrasoma flavescens</i> (yellow tang)	622.69	<i>Rhinomuraena quaesita</i> (ribbon moray)	1.33
	Lissamphibia	15.83	<i>Hyla regilla</i> (tree frog)	242.50	<i>Amphiuma tridactylum</i> (amphiuma)	1.19
	Squamata	27.89	<i>Phrynosoma taurus</i> (horned lizard)	330.32	<i>Lampropeltis getula</i> (kingsnake)	1.07
	Aves	59.42	<i>Gallus gallus</i> (chicken)	185.03	<i>Recurvirostra americana</i> (avocet)	0.49
	Mammalia	60.50	<i>Chinchilla lanigera</i> (chinchilla)	196.75	<i>Balaenoptera musculus</i> (blue whale)	0.51
Secondary body axis	Actinopterygii	1.40	<i>Balistes vetula</i> (triggerfish)	102.50	<i>Myrophis vafer</i> (worm eel)	1.87
	Lissamphibia	2.21	<i>Hyla versicolor</i> (tree frog)	42.44	<i>Amphiuma tridactylum</i> (amphiuma)	1.28
	Squamata	1.84	<i>Phrynosoma taurus</i> (horned lizard)	71.67	<i>Lampropeltis getula</i> (kingsnake)	1.59
	Aves	0.78	<i>Sula leucogaster</i> (brown booby)	6.49	<i>Recurvirostra americana</i> (avocet)	0.92
	Mammalia	0.68	<i>Procyon lotor</i> (raccoon)	11.62	<i>Bassariscus astutus</i> (ring-tailed cat)	1.23
Head	Actinopterygii	4.96	<i>Moringua javanica</i> (spaghetti eel)	303.39	<i>Strongylura marina</i> (needlefish)	1.79
	Lissamphibia	5.61	<i>Hyla regilla</i> (tree frog)	27.73	<i>Ambystoma mexicanum</i> (axolotl)	0.69
	Squamata	6.96	<i>Phrynosoma taurus</i> (horned lizard)	55.09	<i>Boa constrictor</i> (boa)	0.90
	Aves	16.90	<i>Crax rubra</i> (curassow)	129.44	<i>Recurvirostra americana</i> (avocet)	0.88
	Mammalia	8.00	<i>Paradicticus potto</i> (potto)	145.25	<i>Balaenoptera musculus</i> (blue whale)	1.26
Precaudal	Actinopterygii	6.12	<i>Zebrasoma flavescens</i> (yellow tang)	315.40	<i>Moringua edwardsi</i> (spaghetti eel)	1.71
	Lissamphibia	6.91	<i>Hyla regilla</i> (tree frog)	107.80	<i>Dermophis mexicanus</i> (caecilian)	1.19
	Squamata	6.86	<i>Phyllodactylus baurii</i> (leaf-toed gecko)	211.20	<i>Charina bottae</i> (rubber boa)	1.49
	Aves	25.10	<i>Tyto alba</i> (barn owl)	63.28	<i>Anas acuta</i> (pintail)	0.40
	Mammalia	8.30	<i>Perameles nasuta</i> (bandicoot)	58.37	<i>Capra nubiana</i> (ibex)	0.85
Caudal	Actinopterygii	8.19	<i>Elacatinus horsti</i> (goby)	440.00	<i>Rhinomuraena quaesita</i> (ribbon eel)	1.73
	Lissamphibia	0.00	<i>Hyla & Rana</i> (frogs)	148.75	<i>Ambystoma californiense</i> (salamander)	2.17
	Squamata	10.14	<i>Phrynosoma taurus</i> (horned lizard)	225.56	<i>Lacerta trilineata</i> (green lizard)	1.35
	Aves	4.00	<i>Amazona auropalliata</i> (parrot)	21.36	<i>Spheniscus humboldti</i> (penguin)	0.73
	Mammalia	9.67	<i>Ursus malayanus</i> (sun bear)	76.39	<i>Felis pardus</i> (leopard)	0.90

^a Range given in orders of magnitude (=log₁₀(max) – log₁₀(min)).

neither head elongation nor secondary axis reduction contributed much independently to VSI (Fig. 5), suggesting that diversity in the degree of elongation in anguilliform eels is a product of variation in the axial skeleton alone. Indeed, precaudal elongation and caudal elongation are strongly positively associated in Anguilliformes ($r=0.43$, $P=0.008$; Table 2). In blennioids, variation in head elongation contributes independently to VSI (9%), but the vast majority of VSI variation is shared among anatomical components (76%; Fig. 5). Strong positive associations between precaudal elongation and caudal elongation ($r=0.59$, $P<0.001$) and between caudal elongation and secondary axis reduction ($r=0.69$, $P<0.001$) are evident in blennioids (Table 2).

Lissamphibia: Lissamphibians exhibit a smaller range of VSI than ray-finned fishes, but the compact-bodied frogs (*Hyla* and

Rana species, VSI range = 15.8–32.4) exhibit the lowest VSI values of any vertebrate in our data set. As adults, anurans lose the caudal region of the axial skeleton, resulting in caudal elongation values of 0. In addition, frogs exhibit the lowest values among lissamphibians for the other anatomical components (Table 1). *Amphiuma* (*Amphiuma tridactylum*, VSI = 242.5) represents the upper extreme of VSI for Lissamphibians, followed by the tiger salamander (*Ambystoma californiense*, VSI = 187.8) and the Pacific giant salamander (*Dicamptodon ensatus*, VSI = 172.3). Surprisingly, these salamanders have larger VSI values than the eel-like caecilian (*Dermophis mexicanus*, VSI = 137.4) and the slender salamander (*Batrachoseps attenuatus*, VSI = 120.9), though the latter two species are in the upper 50% of the VSI distribution for all vertebrates. In spite of large values for precaudal elongation (=107.8) and

Table 2
Correlation matrices for VSI components by vertebrate clade.

Taxon	N	Trait	Head	Precaudal	Caudal
Actinopterygii	113	Secondary body axis	0.16	0.49***	0.35***
		Head	–	0.01	–0.04
		Precaudal	–	–	0.68***
Anguilliformes	36	Secondary body axis	–0.07	0.36*	0.09
		Head	–	0.03	0.18
		Precaudal	–	–	0.43**
Blennioidei	33	Secondary body axis	0.17	0.25	0.69***
		Head	–	0.23	0.08
		Precaudal	–	–	0.59***
Lissamphibia	14	Secondary body axis	–0.19	0.87***	0.30
		Head	–	–0.16	–0.19
		Precaudal	–	–	0.17
Squamata	14	Secondary body axis	0.37	0.69**	–0.14
		Head	–	0.14	–0.28
		Precaudal	–	–	–0.46
Aves	11	Secondary body axis	0.25	–0.03	0.14
		Head	–	0.11	–0.04
		Precaudal	–	–	0.52
Mammalia	35	Secondary body axis	–0.12	–0.07	0.55***
		Head	–	–0.12	–0.17
		Precaudal	–	–	0.13

* $0.01 \leq P < 0.05$.

** $0.001 \leq P < 0.01$.

*** $P < 0.001$.

secondary axis reduction (=21.0), caecilians have few caudal vertebrae (Wake, 1980; Woltering et al., 2009), resulting in less extreme VSI values. Although the slender salamander is in the 90th percentile for secondary axis reduction, it is unexceptional in terms of axial skeleton elongation and head elongation.

VSI variation in Lissamphibia is primarily explained by caudal elongation (42%; Fig. 4), which makes sense given that some lissamphibians have lost the caudal vertebral region entirely and others have relatively long tails (Wake, 1966; Handrigan and Wassersug, 2007). Indeed, of the five vertebrate clades we examined, lissamphibians have the largest range of caudal elongation (more than two orders of magnitude; Table 1). Just over 50% of VSI variation is shared among components. This result is largely a consequence of a strong, positive correlation between precaudal elongation and secondary axis reduction ($r=0.87$, $P<0.001$). In addition, the correlation between caudal elongation and secondary axis reduction is nearly as strong as the one estimated for ray-finned fishes ($r=0.30$, $P=0.30$; Table 2), though this correlation coefficient is non-significant, probably because of limited sample size.

Squamata: Squamates are also highly diverse in body shape, exhibiting more than an order of magnitude range in VSI (Table 1). At the stout-bodied extreme are the horned lizard (*Phrynosoma taurus*, VSI=27.9) and alligator lizard (*Elgaria multicarinata*, VSI=47.6). The snakes (kingsnake/*Lampropeltis getula*, VSI=330.3; rubber boa/*Charina bottae*, VSI=298.1; and rattlesnake/*Crotalus atrox*, VSI=275.4) and snake-like lizards (glass lizard/*Ophisaurus apodus*, VSI=231.0; pygopodid/*Lialis jicari*, VSI=212.7) are at the upper end of the VSI distribution. Some other lizards (green lizard/*Lacerta trilineata*, VSI=261.7; green anole/*Anolis carolinensis*, VSI=181.5; leaf-toed gecko/*Phyllodactylus baurii*, VSI=176.5; and five-lined skink/*Eumeces fasciatus*, VSI=174.6) are also in the upper 75th percentile of VSI, probably because of their long tails and large caudal elongation values (range=119.1–225.6).

Both precaudal elongation and caudal elongation are important independent contributors to VSI diversity in squamates (26 and 34%, respectively), while head elongation and secondary axis reduction independently explain very little variation (1.3 and 1.6%, respectively; Fig. 4). More than one third of VSI variation is shared among components. Precaudal elongation is strongly positively correlated with secondary axis reduction ($r=0.69$, $P=0.006$) and negatively associated with caudal elongation ($r=-0.46$, $P=0.09$; Table 2), though this latter correlation coefficient is marginally non-significant.

Mammalia: Mammals span only about half an order of magnitude in VSI, a much smaller range than ray-finned fishes, lissamphibians or squamates (Table 1). In addition, mammals tend to be intermediate in VSI. Only four of the 35 sampled species extend beyond the mid-50% interval of the vertebrate VSI distribution (Fig. 3); the dog (*Canis familiaris*, VSI=66.5) and hedgehog (*Erinaceus europaeus*, VSI=69.3) are at the lower end, while the blue whale (*Balaenoptera musculus*, VSI=196.8) and leopard (*Felis pardus*, VSI=159.1) are at the upper end. Despite their limited VSI range, mammals exhibit the second largest range of head elongation, a result largely driven by the largest animal on earth, the blue whale (*B. musculus*), which has the second-most elongate skull (head elongation=145.3) of any vertebrate we measured.

Head elongation is the most important explanatory variable of mammalian body shape diversity, independently accounting for 42% of VSI variation. However, precaudal elongation and caudal elongation also make substantial independent contributions (15 and 21%, respectively). The percentage of VSI variation shared among components is low (21%), and correlations among components are mostly weak; only caudal elongation and secondary axis reduction are correlated ($r=0.55$, $P<0.001$; Table 2).

Aves: Similar to the mammals, our sample of birds exhibits a limited range of VSI values (0.49 orders of magnitude, Table 1)

that are mostly intermediate. Two species possess VSI values in the lower 25th percentile – the chicken (*Gallus gallus*, VSI=59.4) and the parrot (*Amazona auropalliata*, VSI=62.8). Also, two species fall above the 75th percentile – the avocet (*Recurvirostra americana*, VSI=185.0) and the stork (*Mycteria americana*, VSI=167.1).

Head elongation is overwhelmingly the most important anatomical component in birds, independently accounting for 71% of VSI variation (Fig. 3). Because birds are bipedal, however, we note the long axis of the head is not in line with the primary body axis, and long-headedness may not contribute to elongate shape in birds in the same way it does in other vertebrates. Nearly all of the variation in VSI that is not explained by head elongation is shared among multiple components (22%). The correlation between precaudal elongation and caudal elongation was strong but marginally non-significant ($r=0.52$, $P=0.10$) probably because of limited power resulting from small sample size. The remaining correlations among components were weak and non-significant (Table 2).

3.2. Association between VSI and swimming mode in ray-finned fishes

We found significant variation in VSI among the four swimming modes of paired fin propulsion, median fin propulsion, caudal undulation, and body undulation ($F_{3,11}=6.59$, $P=0.008$; see Fig. 6A). As predicted, body undulators, which generate a propulsive wave along a large portion of the body down through the tail, have the largest VSI and are significantly different from caudal undulators and paired fin propulsors ($P=0.022$ and $P=0.009$, respectively), which have a similarly low VSI. The VSI values of body undulators did not, however, differ from those of median fin propulsors ($P=0.401$). ANOVA and pairwise comparisons of anatomical components revealed that the relatively large VSI of body undulators is primarily a result of caudal elongation, which is significantly greater for this swimming mode than any other ($F_{3,11}=7.76$, $P=0.005$; $P[\text{body vs. median fin}]=0.038$; $P[\text{body vs. caudal}]=0.009$; $P[\text{body vs. paired fin}]=0.007$). In addition, median fin swimmers exhibit greater head elongation than any other swimming mode ($F_{3,11}=10.88$, $P=0.001$; $P[\text{median fin vs. body}]=0.006$; $P[\text{median fin vs. caudal}]=0.002$; $P[\text{median fin vs. paired fin}]=0.002$), suggesting that fishes using their median fins for swimming have larger VSI values than caudal undulators and paired fin propulsors because of their relatively long heads.

4. Discussion

We present VSI as a metric of body shape in vertebrates that separates stout-bodied from elongate forms by summing four distinct anatomical components: secondary axis reduction, head elongation, precaudal elongation and caudal elongation. VSI, therefore, allows for both quantification of body shape diversity and identification of the anatomical basis of that diversity. Whereas several metrics are well suited for quantifying body shape along the elongation continuum (e.g., elongation ratio [Ward and Azizi, 2004]; fineness ratio [Webb, 1975]; body aspect ratio [Helfman et al., 2009]), only axial elongation index (AEI; Ward and Brainerd, 2007) and VSI (Table 1 and Fig. 3) achieve this goal by incorporating measurements of morphological structures that contribute to shape variation. We view VSI as a necessary revision of AEI because VSI incorporates head shape and reduction of the secondary body axis in addition to regional elongation of the axial skeleton. We show that while axial elongation is the primary contributor to shape variation in ray-finned fishes, lissamphibians and squamates, head elongation is of major importance to birds and mammals (Fig. 4). This variation among clades illustrates that incorporating detailed morphological measurements into shape metrics

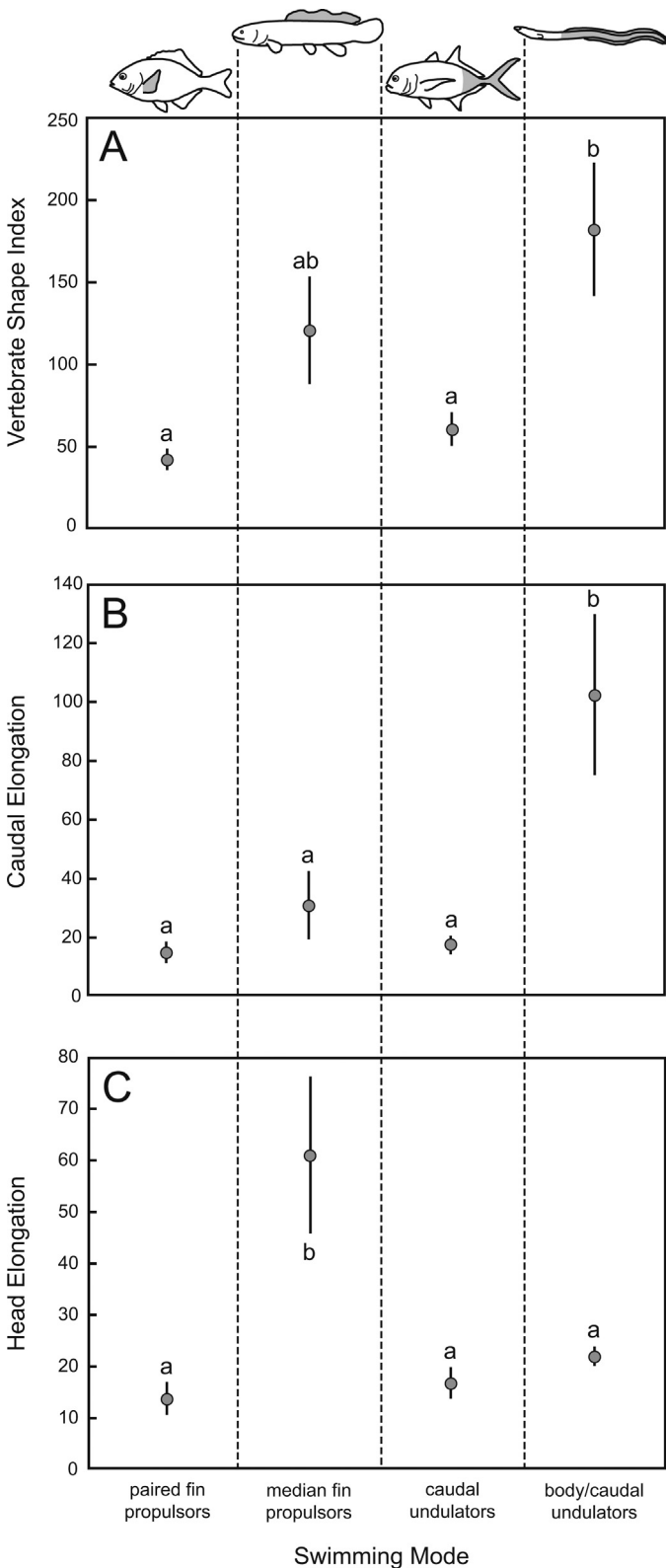


Fig. 6. Comparisons of (A) vertebrate shape index (VSI), (B) caudal elongation, and (C) head elongation among four swimming modes in ray-finned fishes. Values are means and error bars represent \pm standard error. Letter combinations (a, b, ab) indicate statistical significance of differences between pairs of swimming modes at $\alpha = 0.05$ by Tukey's HSD.

provides important insights into the anatomical basis of shape variation and further suggests that anatomical features beyond the axial skeleton should be examined. The advantage of VSI over other shape metrics is that it more comprehensively captures variation in the morphological features that make an organism more or less elongate.

In this study, we collected data on 194 vertebrate species spanning Actinopterygii, Lissamphibia, Testudines, Squamata, Crocodylia, Aves and Mammalia to show how the morphological traits that comprise VSI can be readily measured on a variety of skeletal preparations, including cleared and stained, dry skeletal, and radiographed specimens. We specify methods for measuring these traits with the aim of ensuring that values taken from different specimen types – particularly two- and three-dimensional preparations – correspond with one another. VSI's versatility with respect to its quantification on various specimen types is not unique among body shape metrics; ER and AEI can also be measured on the preparations examined in this study. Nevertheless, correspondence between measurements on different specimen types is critical to any metric's use in large-scale comparisons of body shape because preparation techniques may vary among taxa; all three preparations are relatively common in fishes, lissamphibians and squamates, but mammal and bird preparations are generally dry skeletons (see Table S1 in the supplementary online Appendix A).

Our data show that VSI captures shape variation along the elongation continuum, as we intended. Vertebrates span more than 1.5 orders of magnitude in VSI, from the tree frog to the ribbon moray (Table 1 and Fig. 3). The lower extreme of the VSI distribution comprises several compact-bodied forms sampled from different vertebrate orders, including frogs, the horned lizard, and several coral reef fishes. The upper extreme of VSI is predominantly populated by the true eels – 15 of the 20 species with the largest VSI values are from the Anguilliformes (Fig. 3) – but also includes a lissamphibian (amphiuma) and several squamates (snakes, snake-like lizards). We note that other shape metrics likely perform just as well as VSI in terms of describing variation along this continuum. In fact, two of these metrics, ER and AEI, are components of VSI and are therefore highly correlated with it ($r_{VSI \times ER} = 0.57$; $r_{VSI \times AEI} = 0.95$). We present these results simply to show that VSI does in fact describe the axis of variation for which we designed it.

4.1. VSI diversity in vertebrate clades

Because VSI involves measurements of morphological traits shared across vertebrates, it can be used to compare body shape diversity among any set of vertebrate taxa. To illustrate this application of VSI, we show that five major vertebrate clades display varying degrees of shape diversity (Table 1 and Fig. 3). We found the greatest range of VSI within Actinopterygii, and this result seems to be a consequence of several anguilliform eels possessing greater VSI values than any other vertebrate in our data set. Although intermediate in range, both Lissamphibia and Squamata span more than an order of magnitude and include species with lower VSI values than any of the ray-finned fishes. Compared to these shape-diverse clades, Aves and Mammalia have limited VSI ranges, and species from these clades generally possess intermediate VSI values.

We recognize, of course, that our sampling is highly uneven, potentially confounding the rank order of ranges among clades. While Actinopterygii has the largest range, it also comprises the majority of species in our data set. Despite their limited sample sizes, however, lissamphibians and squamates span nearly the same range as ray-finned fishes (90 and 80%, respectively). In addition, we note that our sample may have excluded some species that would further extend the ranges of some clades. This may be particularly true of mammals – we were unable to sample groups known to have elongated precaudal vertebrae (e.g., the giraffe) and greatly

reduced caudal vertebral numbers (e.g., hominoid primates). In addition, our sample of birds left out many diving birds and long-necked wading birds. Nevertheless, we view our sample as a pilot data set sufficient for demonstrating the utility of VSI, rather than one allowing critical evaluation of differences in diversity among vertebrate taxa.

4.2. Importance of anatomical components to VSI variation

Variation in elongation of the caudal axial skeleton is of major importance to vertebrate body shape diversity. Caudal elongation accounts for the greatest proportion of VSI variation within Actinopterygii, Lissamphibia, and Squamata – the clades with the largest ranges in VSI. Although head elongation explains the largest proportion of VSI in Mammalia, caudal elongation is a prominent explanatory component as well. Aves is the only clade in which caudal elongation accounts for little VSI variation.

We found that head elongation contributes to a large proportion of shape variation in mammals and birds and a lesser but substantial proportion in ray-finned fishes and squamates (Fig. 4). Combined with our finding that head elongation exhibits weak correlations with other VSI components (Table 2), these results reveal that head elongation is an important independent source of vertebrate shape diversity, validating VSI as a revision of AEI that incorporates this component. Moreover, the weak correlations between head elongation and precaudal elongation or caudal elongation allay concerns that standardization of head length by the vertebral length would introduce a correlation between these components.

Precaudal elongation contributes nearly as much as caudal elongation to shape diversity in squamates and mammals but independently explains only about 5% of VSI in the other three clades (Fig. 4). The limited explanatory ability of precaudal elongation in ray-finned fishes, lissamphibians and squamates appears to be a result of its correlations with other components, particularly secondary axis reduction (Table 2).

Secondary axis reduction makes little independent contribution to VSI variation within any of the five clades (Fig. 4). This result appears to be a consequence of the strong association between secondary axis reduction and axial skeleton elongation; secondary axis reduction is strongly correlated with precaudal elongation or caudal elongation in four of the five clades we examined (Table 2). Despite its minor explanatory role, however, we take a conservative approach in retaining secondary axis reduction as part of VSI because it remains a potential independent axis for shape change. Secondary axis reduction may be more important in explaining smaller-scale differences in body shape (Lindsey, 1975), perhaps in a sample of more closely related species that vary less in axial elongation than the disparate species sampled in this study or in an ontogenetic series in a single species.

Our results clarify the importance of different anatomical regions to body shape variation, but previous research into this question has revealed that, even within these regions, elongation may occur through varying suites of morphological changes. For example, variation in elongation of regions of the axial skeleton may arise because of differences in vertebral number, vertebral shape, or both (Parra-Olea and Wake, 2001; Ward and Brainerd, 2007; Bergmann and Irschick, 2012). To examine finer-scale morphological differences underlying body shape diversity, head elongation, precaudal elongation, and caudal elongation can be further decomposed into the morphological traits that comprise them (see Eq. (2)). Both precaudal elongation and caudal elongation are products of regional vertebral counts and their aspect ratios, and these facets of the axial skeleton may vary independently (Ward and Brainerd, 2007). To determine the basis for elongation within a region of the axial skeleton, precaudal elongation or caudal elongation could be regressed (as the dependent variable) against

vertebral number and aspect ratio. For example, within ray-finned fishes, caudal vertebral number, N_{CV} , independently accounts for more variation in caudal elongation than caudal aspect ratio, AR_{CV} , by a factor of 1.4 (N_{CV} and AR_{CV} independently account for 56 and 39%, respectively, based on least squares linear regression of log-transformed data). Similarly, regressing head elongation against its morphological determinants (head length standardized by vertebral length, $L_{head\ in\ vertebrae}$, and head aspect ratio, AR_{head}) would allow partitioning the effects of head size and shape. In this way, VSI can be applied to identify the anatomical basis of body shape variation at the level of body region (head, precaudal, caudal, or secondary axis) and at the finer-scale level of individual morphological traits.

4.3. VSI and swimming mode in ray-finned fishes

We found only some support for the predicted association between body elongation and swimming mode. Although body undulators (i.e., anguilliform swimmers) follow the predicted pattern and had significantly greater VSI values than fishes of any other swimming mode, caudal undulators (i.e., carangiform, subcarangiform and thunniform swimmers) have VSI values nearly as low as paired fin propulsors (Fig. 6). The morphological components of VSI are also nearly identical in caudal undulators and paired fin propulsors. Most notable is their similar values of caudal elongation – the region that bends during caudal-based swimming (Fig. 6). We speculate on two possible, non-exclusive reasons for this result. First, caudal undulators may be less elongate than predicted because the majority of the axial skeleton remains rigid during caudal undulation, favoring fewer vertebrae (Long and Nipper, 1996) and less axial elongation. Moreover, caudal swimmers utilize lower-amplitude undulations compared to anguilliform swimmers (Tytell et al., 2010), and bending at the tail region may require little or no elongation of the body or caudal region. Second, paired fin propulsors may be more elongate than predicted because of factors unrelated to steady swimming. Although the body and caudal fin do not undulate during steady swimming, many paired fin-based swimmers bend axially during turns. If more elongate forms are able to bend and turn more tightly, turning performance may also affect body elongation (Brainerd and Patek, 1998; Porter et al., 2009; Long et al., 2010). Indeed, the majority of paired fin propulsors in our data set occupy coral reefs, where maneuverability is important in navigating a structurally complex environment (Fulton and Bellwood, 2002; Fulton et al., 2005).

Median fin propulsors exhibited intermediate VSI values, though this result provides only limited support for the hypothesis that elongation enhances performance of this swimming mode through lengthening of the dorsal and/or anal fin. This swimming mode has the second highest mean values for precaudal elongation and caudal elongation, but it is highly variable in these components and does not differ significantly from those of the less elongate caudal undulators or paired fin swimmers. Although lengthening the median fin along the body remains a possibility (Ward and Mehta, 2010), these results suggest that median fin swimmers do not consistently elongate their axial skeleton to expand the median fin. Instead, increased head elongation explains the intermediate VSI of median fin swimmers (Fig. 6). We speculate that elongate heads may be a consequence of some other selective demand rather than swimming mode because we are unaware of any mechanism that would link head elongation and median fin-based swimming performance.

4.4. Extensions

As a revised metric of body shape that varies between stout-bodied and elongate forms, VSI can be applied to investigate a

variety of questions concerning how body shape evolves and the biological consequences of disparate forms. Because VSI can be measured for any vertebrate taxon, it may be a particularly effective metric for examining convergence in body shape. By identifying taxa that converge in VSI and testing associations with ecological variables like habitat and diet, future research may shed light on the ecological selective demands underlying body shape transformations (Wiens et al., 2006; Bergmann et al., 2009; Yamada et al., 2009). Moreover, because VSI also provides insights into the anatomical basis of body shape differences, one can ask whether the same suite of morphological changes underlies transitions in shape in different taxa. This type of study would provide insights into the roles of contingency and constraint on body shape evolution. In addition, one could quantify VSI widely across vertebrates to investigate proposed relationships between body shape evolution and modifications to the appendicular skeleton or specific aspects of the skull. For example, the association between elongation and reduction or loss of appendages could be quantified across squamates, lissamphibians and ray-finned fishes. Lastly, we point out that in the rare instances when intact fossils are obtained, VSI can shed light on the anatomical basis of body shape in extinct taxa as well. With the increasing availability of both phylogenetic hypotheses for large numbers of vertebrate species (e.g., Bininda-Emonds et al., 2007; Wiens, 2011; Wainwright et al., 2012; Wiens et al., 2012) and methods for combining phylogenetic and phenotypic information (e.g., Felsenstein, 1985; Garland et al., 1992; Hansen, 1997; Butler and King, 2004; O'Meara et al., 2006; Revell and Collar, 2009; Beaulieu et al., 2012), we propose that VSI will be a useful metric for advancing study of the evolution of body shape diversity in vertebrates.

Acknowledgements

We thank the following museum curators for access to specimens: J. Dines, curator of Mammalogy, Los Angeles County Museum of Natural History (LACM); K. Garrett, curator of Ornithology, LACM; J. Vindum, curator of Herpetology, California Academy of Sciences (CAS); D. Catania, curator of Ichthyology, CAS. We are grateful to D. Casper, D. Colbin, K. Galloway, L. Miller, and J. Sharick for help with specimen preparation. We also thank J. Fong and CAS for access to X-ray facilities. This work was supported by NSF grants IOS 0819009 and REU 1126349 to RSM.

Appendix A. Supplementary data

Supplementary data associated with this article can be found, in the online version, at <http://dx.doi.org/10.1016/j.zool.2013.03.001>.

References

- Adams, D.C., Rohlf, F.J., Slice, D.E., 2004. Geometric morphometrics: ten years of progress following the 'revolution'. *Ital. J. Zool.* 71, 5–16.
- Adams, D.C., Berns, C.M., Kozak, K.H., Wiens, J.J., 2009. Are rates of species diversification correlated with rates of morphological evolution? *Proc. R. Soc. B* 276, 2729–2738.
- Asano, H., 1977. On the tendencies of differentiation in the composition of the vertebral number of teleostean fishes. *Mem. Fac. Agric. Kinki Univ.* 10, 29–37.
- Beaulieu, J.M., Jhvueng, D.-Ch., Boettiger, C., O'Meara, B.C., 2012. Modeling stabilizing selection: expanding the Ornstein–Uhlenbeck model of adaptive evolution. *Evolution* 66, 2369–2383.
- Bergmann, P.J., Irschick, D.J., 2012. Vertebral evolution and diversification of squamate reptiles. *Evolution* 66, 1044–1058.
- Bergmann, P.J., Myers, J.J., Irschick, D.J., 2009. Directional evolution of stockiness coevolves with ecology and locomotion in lizards. *Evolution* 63, 215–227.
- Bininda-Emonds, O.R.P., Cardillo, M., Jones, K.E., MacPhee, R.D.E., Beck, R.M.D., Grenyer, R., Price, S.A., Vos, R.A., Gittleman, J.L., Purvis, A., 2007. The delayed rise of present-day mammals. *Nature* 446, 507–512.
- Blomberg, S.P., Garland Jr., T., Ives, A.R., 2003. Testing for phylogenetic signal in comparative data: behavioral traits are more labile. *Evolution* 57, 717–745.
- Brainerd, E.L., Patek, S.N., 1998. Vertebral column morphology, C-start curvature, and the evolution of mechanical defenses in tetraodontiform fishes. *Copeia* 1998, 971–984.
- Brandley, M.C., Huelsenbeck, J.P., Wiens, J.J., 2008. Rates and patterns in the evolution of snake-like body form in squamate reptiles: evidence for repeated re-evolution of lost digits and long-term persistence of intermediate body forms. *Evolution* 62, 2042–2064.
- Butler, M.A., King, A.A., 2004. Phylogenetic comparative analysis: a modeling approach for adaptive evolution. *Am. Nat.* 164, 683–695.
- Felsenstein, J., 1985. Phylogenies and the comparative method. *Am. Nat.* 125, 1–15.
- Freckleton, R.P., Harvey, P.H., Pagel, M., 2002. Phylogenetic analysis and comparative data: a test and review of evidence. *Am. Nat.* 160, 712–726.
- Fulton, C.J., Bellwood, D.R., 2002. Patterns of foraging in labrid fishes. *Mar. Ecol. Prog. Ser.* 226, 135–142.
- Fulton, C.J., Bellwood, D.R., Wainwright, P.C., 2005. Wave energy and swimming performance shape coral reef fish assemblages. *Proc. R. Soc. B* 272, 827–832.
- Gans, C., 1975. Tetrapod limblessness: evolution and functional corollaries. *Am. Zool.* 15, 455–467.
- Garland Jr., T., Harvey, P.H., Ives, A.R., 1992. Procedures for the analysis of comparative data using phylogenetically independent contrasts. *Syst. Biol.* 41, 18–32.
- Grande, L., Bemis, W.E., 1998. A comprehensive phylogenetic study of amiid fishes (Amiidae) based on comparative skeletal anatomy. An empirical search for interconnected patterns of natural history. *J. Vert. Paleont.* 18, 1–690.
- Handrigan, G.R., Wassersug, R.J., 2007. The anuran Bauplan: a review of the adaptive, developmental, and genetic underpinnings of frog and tadpole morphology. *Biol. Rev.* 82, 1–25.
- Hansen, T.F., 1997. Stabilizing selection and the comparative analysis of adaptation. *Evolution* 51, 1341–1351.
- Helfman, G.S., Collette, B.B., Facey, D.E., Bowen, B.W., 2009. *The Diversity of Fishes: Biology, Evolution, and Ecology*, 2nd ed. Blackwell Science, Malden, MA.
- Johnson, R.G., 1955. The adaptive and phylogenetic significance of vertebral form in snakes. *Evolution* 9, 367–388.
- Langerhans, R.B., Gifford, M.E., Joseph, E.O., 2007. Ecological speciation in *Gambusia* fishes. *Evolution* 61, 2056–2074.
- Liem, K.F., Bemis, W.E., Walker Jr., W.F., Grande, L., 2001. *Functional Anatomy of the Vertebrates: An Evolutionary Perspective*. Harcourt College Publishers, Philadelphia.
- Lindsey, C.C., 1975. Pleomerism, widespread tendency among related fish species for vertebral number to be correlated with maximum body length. *J. Fish Res. Board Can.* 32, 2453–2469.
- Lindsey, C.C., 1978. Form, function, and locomotory habits in fish. In: Hoar, W.S., Randall, D.J. (Eds.), *Fish Physiology*, vol. VII. Academic Press, Waltham, MA, pp. 1–98.
- Long Jr., J.H., Nipper, K.S., 1996. The importance of body stiffness in undulatory propulsion. *Am. Zool.* 36, 678–694.
- Long Jr., J.H., Porter, M.E., Root, R.G., Liew, C.W., 2010. Go reconfigure: how fish change shape as they swim and evolve. *Integr. Comp. Biol.* 50, 1120–1139.
- Losos, J.B., 1990. Ecomorphology, performance capability, and scaling of West Indian *Anolis* lizards: an evolutionary analysis. *Ecol. Monog.* 60, 369–388.
- Mehta, R.S., Ward, A.B., Alfaro, M.E., Wainwright, P.C., 2010. Elongation of the body in eels. *Integr. Comp. Biol.* 50, 1091–1105.
- Müller, J., Scheyer, T.M., Head, J.J., Barrett, P.M., Werneberg, I., Ericson, P.G.P., Pol, D., Sánchez-Villagra, M.R., 2010. Homeotic effects, somitogenesis and the evolution of vertebral numbers in recent and fossil amniotes. *Proc. Natl. Acad. Sci. U.S.A.* 107, 2118–2123.
- Nelson, J.S., 2006. *Fishes of the World*, 4th ed. John Wiley and Sons, New York.
- O'Meara, B.C., Ané, C., Sanderson, M.J., Wainwright, P.C., 2006. Testing for different rates of continuous trait evolution using likelihood. *Evolution* 60, 922–933.
- Parra-Olea, G., Wake, D.B., 2001. Extreme morphological and ecological homoplasy in tropical salamanders. *Proc. Natl. Acad. Sci. U.S.A.* 98, 7888–7891.
- Polly, P.D., Head, J.J., Cohn, M.J., 2001. Testing modularity and dissociation: the evolution of regional proportions in snakes. In: Zelditch, M.L. (Ed.), *Beyond Heterochrony: The Evolution of Development*. Wiley-Liss Inc., New York, pp. 305–335.
- Porter, M.E., Roque, C.M., Long Jr., J.H., 2009. Turning maneuvers in sharks: predicting body curvature from axial morphology. *J. Morphol.* 270, 954–965.
- Pough, H.F., Andrews, R.M., Cadle, J.E., Crump, M.L., Savitzky, A.H., Wells, K.D., 1998. *Body support and locomotion*. In: Pough, H.F. (Ed.), *Herpetology*. Prentice Hall, Englewood Cliffs, NJ (Chapter 8).
- Pough, F.H., Janis, C.M., Heiser, J.B., 2009. *Vertebrate Life*, 8th ed. Benjamin Cummings, San Francisco.
- R Development Core Team, 2012. *R: A Language and Environment for Statistical Computing*. R Foundation for Statistical Computing, Vienna, Austria.
- Revell, L.J., Collar, D.C., 2009. Phylogenetic analysis of the evolutionary correlation using likelihood. *Evolution* 63, 1090–1100.
- Richardson, M.K., Allen, S.P., Wright, G.M., Raynaud, A., Hanken, J., 1998. Somite number and vertebral evolution. *Development* 125, 151–160.
- Rohlf, F.J., 2006. A comment on phylogenetic correction. *Evolution* 60, 1509–1515.
- Rohlf, F.J., Marcus, L.F., 1993. A revolution in morphometrics. *Trends Ecol. Evol.* 8, 129–132.
- Rüber, L., Adams, D.C., 2001. Evolutionary convergence of body shape and trophic morphology in cichlids from Lake Tanganyika. *J. Evol. Biol.* 14, 325–332.
- Tytell, E.D., Borazjani, I., Sotiropoulos, F., Baker, T.V., Andersos, E.J., Lauder, G.V., 2010. Disentangling the functional roles of morphology and motion in the swimming of fish. *Integr. Comp. Biol.* 50, 1140–1154.

- Wainwright, P.C., Smith, W.L., Price, S.A., Tang, K.L., Sparks, J.S., Ferry, L.A., Kuhn, K.L., Eytan, R.I., Near, T.J., 2012. The evolution of pharyngognath: a phylogenetic and functional appraisal of the pharyngeal jaw key innovation in Labroid fishes and beyond. *Syst. Biol.* 61, 1001–1027.
- Wake, D.B., 1966. Comparative osteology and evolution of the lungless salamander, family Plethodontidae. *Mem. S. Cal. Acad. Sci.* 4, 1–111.
- Wake, M.H., 1980. Morphometrics of the skeleton of *Dermophis mexicanus* (Amphibia: Gymnophiona). Part I. The vertebrae, with comparisons to other species. *J. Morphol.* 165, 117–130.
- Walker, J.A., Bell, M.A., 2000. Net evolutionary trajectories of body shape evolution within a microgeographic radiation of threespine sticklebacks (*Gasterosteus aculeatus*). *J. Zool. Lond.* 252, 293–302.
- Ward, A.B., Azizi, E., 2004. Convergent evolution of the head retraction escape response in elongate fishes and amphibians. *Zoology* 107, 205–217.
- Ward, A.B., Brainerd, E.L., 2007. Evolution of axial patterning in elongate fishes. *Biol. J. Linn. Soc.* 90, 97–116.
- Ward, A.B., Kley, N.J., 2012. Effects of precaudal elongation on visceral topography in a basal clade of ray-finned fishes. *Anat. Rec.* 295, 289–297.
- Ward, A.B., Mehta, R.S., 2010. Axial elongation in fishes: using morphological approaches to elucidate developmental mechanisms in studying body shape. *Integr. Comp. Biol.* 50, 110–1119.
- Webb, P.W., 1975. Hydrodynamics and energetics of fish propulsion. *Bull. Fish Res. Board Can.* 190, 1–159.
- Webb, P.W., 1982. Locomotor patterns in the evolution of actinopterygian fishes. *Am. Zool.* 22, 329–342.
- Wiens, J.J., 2011. Re-evaluation of lost mandibular teeth in frogs after more than 200 million years, and re-evaluating Dollo's law. *Evolution* 65, 75–96.
- Wiens, J.J., Brandley, M.C., Reeder, T.W., 2006. Why does a trait evolve multiple times within a clade? Repeated evolution of snakelike body form in squamate reptiles. *Evolution* 60, 123–141.
- Wiens, J.J., Hutter, C.R., Mulcahy, D.G., Noonan, B.P., Townsend, T.M., Sites Jr., J.W., Reeder, T.W., 2012. Resolving the phylogeny of lizards and snakes (Squamata) with extensive sampling of genes and species. *Biol. Lett.* 8, 1043–1046.
- Woltering, J.M., Vonk, F.J., Müller, H., Bardine, N., Tuduze, I.L., de Bakker, M.A.G., Knöchel, W., Sirbu, I.O., Durston, A.J., Richardson, M.K., 2009. Axial patterning in snakes and caecilians: evidence for alternative interpretation of the *Hox* code. *Dev. Biol.* 332, 82–89.
- Yamada, T., Sugiyama, T., Tamaki, N., Kawakita, A., Kato, M., 2009. Adaptive radiation of gobies in the interstitial habitats of gravel beaches accompanied by body elongation and excessive vertebral segmentation. *BMC Evol. Biol.* 91, 145.
- Yamahira, K., Nishida, T., 2009. Latitudinal variation in axial patterning of the medaka (Actinopterygii: Adrianichthyidae): Jordan's rule is substantiated by genetic variation in abdominal vertebral number. *Biol. J. Linn. Soc.* 96, 856–866.